Delayed Buckling and Guided Folding of Inhomogeneous Capsules

Sujit S. Datta,[1] Shin-Hyun Kim,[2,3] Jayson Paulose,[2] Alireza Abbaspourrad,[2] David R. Nelson,[1] and David A. Weitz[1,2]

[1]*Department of Physics, Harvard University, Cambridge, Massachusetts 02138, USA*
[2]*Harvard School of Engineering and Applied Sciences, Cambridge, Massachusetts 02138, USA*
[3]*Department of Chemical and Biomolecular Engineering, KAIST, Daejeon, South Korea*

Colloidal capsules can sustain an external osmotic pressure; however, for a sufficiently large pressure, they will ultimately buckle. This process can be strongly influenced by structural inhomogeneities in the capsule shells. We explore how the time delay before the onset of buckling decreases as the shells are made more inhomogeneous; this behavior can be quantitatively understood by coupling shell theory with Darcy's law. In addition, we show that the shell inhomogeneity can dramatically change the folding pathway taken by a capsule after it buckles.

PACS numbers: 46.32.+x, 46.70.De, 47.55.D−, 47.56.+r

Many important natural or technological situations require understanding thin, spherical shells; examples include colloidal capsules for chemical encapsulation and release [1–3], biological cells [4,5], pollen grains [6], submersibles [7], chemical storage tanks [8], nuclear containment shells [8], and even the Earth's crust [9]. In many cases, the utility of such a shell critically depends on its response to an externally imposed pressure. For small pressures, a homogeneous, spherical shell, characterized by a uniform thickness, supports a compressive stress, and it shrinks isotropically. Above a threshold pressure, however, this shrinkage becomes energetically prohibitive; instead, the shell buckles, reducing its volume by forming a localized indentation at a random position on its surface. For the case of a homogeneous shell, this threshold pressure can be calculated using a linearized analysis of shell theory [10,11], while the exact morphology of the shell after it buckles requires a full nonlinear analysis [12–14]. However, many shells are inhomogeneous, characterized by spatially varying thicknesses and elastic constants [6,15–18]. Such inhomogeneities can strongly influence how a shell buckles [6,10,19–23]. Unfortunately, despite its common occurrence in real shells, exactly how inhomogeneity influences the onset of buckling, as well as the shell morphology after buckling, remains to be elucidated. A deeper understanding requires careful investigation of the buckling of spherical shells with tunable, well-defined, inhomogeneities.

In this Letter, we use a combination of experiments, theory, and simulation to study the buckling of spherical colloidal capsules with inhomogeneous shells of nonuniform thicknesses. We show that the onset of buckling, above a threshold external osmotic pressure, is well described by shell theory; however, even above this threshold, the capsules do not buckle immediately. We find that the time delay before the onset of buckling decreases as the shells are made more inhomogeneous; these dynamics can be quantitatively understood by coupling shell theory with

Darcy's law for flow through a porous capsule shell, even for highly inhomogeneous shells. Moreover, we find that the shell inhomogeneity guides the folding pathway taken by a capsule during and after buckling. We use these insights to controllably create novel colloidal structures using buckling.

We fabricate monodisperse thin-shelled capsules using water-in-oil-in-water $(W/O/W)$ droplets prepared by microfluidics [24,25]. The inner and outer phases are a 10 wt % solution of polyvinyl alcohol of viscosity $\mu = 13.5$ mPa s, as measured using a strain-controlled rheometer, while the middle oil phase is a photopolymerizable monomer solution. The polyvinyl alcohol solution is less dense than the oil; as a result, after the droplets are produced and collected, the light inner water droplets gradually rise within them. This causes the oil to gradually thin on the top side of each droplet and thicken on the bottom [26]. We exploit this effect to prepare capsules, with outer radius R_0, and spatially varying shell thickness $h(\theta) \approx h_0 - \delta \cos\theta$; θ is measured from the top of the gravitationally oriented shell, h_0 is the average shell thickness, and δ is the total distance moved by the inner droplet, as shown schematically in Fig. 1(a). The shell inhomogeneity can thus be quantified by the ratio δ/h_0. We use UV light to polymerize the oil either as the capsules are produced *in situ*, or after different average waiting times, t_w [27]; this enables us to prepare separate batches of capsules characterized by varying degrees of shell inhomogeneity [28,29]. Some capsules are subsequently washed in deionized water. The shell is a solid characterized by a Young's modulus $E \approx 600$ MPa [30]; importantly, while this shell is impermeable to Na$^+$ and Cl$^-$ ions, it is permeable to water [31].

To probe their mechanical response, we subject inhomogeneous capsules, characterized by $t_w = 1$ min, $\delta/h_0 \approx 0.2$ and $h_0/R_0 = 0.017$, to an external osmotic pressure by injecting and gently mixing 20 μL of the capsule suspension into a fixed volume of NaCl solution,

$V_{NaCl} \approx 130\text{--}400 \ \mu L$. We investigate the pressure depen-
dence of buckling using NaCl concentrations in the range
0.063–2.165 M. Estimating the total volume of the injected
capsules using optical microscopy allows us to calculate
the final NaCl concentration of the outer phase, which
then ranges from $c_{NaCl} = 0.055\text{--}2.068$ M. These corre-
spond to osmotic pressure differences across the shell of
$\Pi = (2c_{NaCl} + \Pi_{out} - \Pi_{in}) \times N_A k_B T = 0.025\text{--}10.09$ MPa,
where N_A is Avogadro's constant, k_B is Boltzmann's con-
stant, $T \approx 300$ K, and Π_{out} and Π_{in} are the measured
osmolarities of the fluids outside and inside the capsules,
respectively, in the absence of NaCl. For each batch of
capsules studied, we monitor an average of 75 capsules
over time using optical microscopy.

The osmotic pressure difference across these inhomoge-
neous shells forces the capsules to buckle; we observe the
abrupt formation of localized indentations in the shells, as
shown in Fig. 1(b). For each osmotic pressure investigated,
the fraction of the capsules that buckle increases over time,
eventually plateauing, as shown in Fig. 1(c). We quantify
this behavior by fitting this increase to an empirical ex-
ponential relationship, exemplified by the smooth lines in
Fig. 1(c). The plateau value of this function yields a
measure of the total fraction of the capsules that ultimately
buckle over sufficiently long times, while the time constant
of this function yields a measure of the time delay before
the onset of buckling, τ. For sufficiently large Π, the total
fraction of the capsules that ultimately buckle increases
dramatically with increasing Π, as shown by the gray
circles in Fig. 1(d); this indicates that the capsules buckle
above a threshold pressure, Π^* [32]. We empirically fit
these data using the cumulative distribution function of a
normal distribution, shown by the black line in Fig. 1(d);
the mean value and standard deviation of this fit yield a
measure of Π^* and the spread in Π^*, respectively.

We study the geometry dependence of Π^* by performing
additional measurements on inhomogeneous capsules,
polymerized *in situ*, with different shell thicknesses and
radii; these are characterized by $\delta/h_0 \approx 0.2$, and $h_0/R_0 =
0.019$ or $h_0/R_0 = 0.1$. Similar to the $h_0/R_0 = 0.017$ case,
for sufficiently large Π, the total fraction of the capsules
that ultimately buckle increases dramatically with increas-
ing Π, as shown by the red triangles and blue squares in
Fig. 1(d). Interestingly, we find that the threshold buckling
pressure $\Pi^* \sim (h_0/R_0)^2$ [Fig. 1(d), inset]; this observation
is reminiscent of the prediction of shell theory for the
buckling of a *uniform* shell [11], despite the fact that our
capsules are inhomogeneous. To understand this behavior,
we consider the local deformability of an inhomogeneous
shell at various points on its surface. Because the 2D
stretching and bending stiffnesses scale as $\sim h$ and $\sim h^3$
[33], respectively, the thinnest part of the shell, where $h \approx
h_0 - \delta$, should be the easiest to deform. We directly visual-
ize that buckling begins at this "weak spot" using confocal
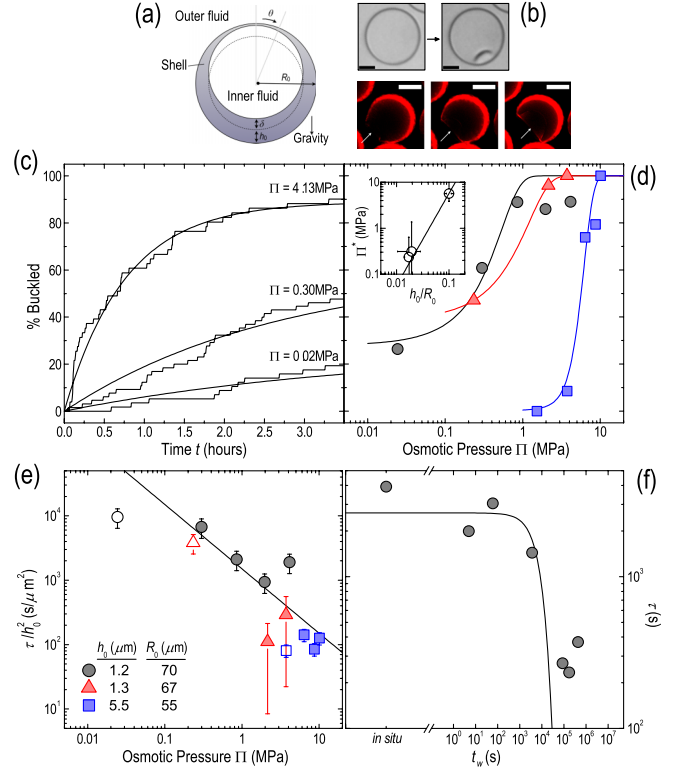microscopy of inhomogeneous capsules with fluorescent

FIG. 1 (color online). (a) Schematic showing the capsule ge-
ometry investigated. (b) Upper: buckling of a capsule; scale bar
is 20 μm. Lower: buckling begins at the thinnest part of the shell
for capsules with thickness inhomogeneity $\delta/h_0 \approx 0.84$; scale
bars are 50 μm. (c) Fraction of capsules buckled over time, for
three different osmotic pressures Π. Capsules have mean shell
thickness $h_0 = 1.2 \ \mu$m, outer radius $R_0 = 70 \ \mu$m, and $\delta/h_0 =
0.20$. Smooth lines show exponential fits. (d) Total fraction of
capsules that ultimately buckle over time for varying Π, for
capsules with h_0, R_0, and $\delta/h_0 = 1.2 \ \mu$m, 70 μm, and 0.20
(gray circles), 1.3 μm, 67 μm, and 0.23 (red triangles), and
5.5 μm, 55 μm, and 0.19 (blue squares). Smooth curves are fits
to the data using the cumulative distribution function of the
normal distribution. Inset shows the mean osmotic pressure of
each fit versus h_0/R_0; vertical and horizontal error bars show the
standard deviation of each fit and estimated variation in h_0/R_0,
respectively. Straight line shows $(h_0/R_0)^2$ scaling. (e) Time
delay before the onset of buckling, τ, normalized by h_0^2, for
varying Π, for the same capsules as in (d). Closed points show
$\Pi > \Pi^*$ while open points show $\Pi < \Pi^*$. Vertical error bars
show uncertainty arising from estimated variation in h_0. Black
line shows Π^{-1} scaling. (f) Time delay τ decreases with the
wait time before a shell is polymerized, t_w; capsules have
$h_0 = 1.2 \ \mu$m and $R_0 = 70 \ \mu$m, and are buckled at $\Pi \approx
0.86$ MPa $> \Pi^*$. Black line shows theoretical prediction cou-
pling shell theory and Darcy's law, as described in the text, with
$k \approx 3.5 \times 10^{-24}$ m^2.

shells characterized by $\delta/h_0 \approx 0.84$ [Fig. 1(b), lower
panel]. Consequently, we expect the onset of buckling to
be governed by deformations in this part of the shell. To
quantify this expectation, we apply shell theory to an
inhomogeneous shell characterized by the same geometry

as the experimental capsules [25]; this analysis yields $\Pi^* = \frac{2E}{\sqrt{3(1-\nu^2)}}(\frac{h_0-\delta}{R_0})^2 \approx 470(h_0/R_0)^2$ MPa, assuming a Poisson ratio $\nu \approx 1/3$. The dependence of Π^* on $h_0 - \delta$ confirms our expectation that the threshold buckling pressure is set by the thinnest part of the inhomogeneous shell. Moreover, we find $\Pi^*(R_0/h_0)^2 \approx 600 \pm 200$ MPa for the experimental capsules [solid line, Fig. 1(d) inset], in good agreement with our theoretical prediction. This indicates that the onset of capsule buckling is well described by shell theory.

Within this framework, for $\Pi > \Pi^*$, a capsule remains spherical before it buckles; it initially responds to the applied pressure by contracting uniformly, reducing its volume from its initial value, V_0, by a threshold amount ΔV^*, before buckling. We find that the time delay before the onset of buckling, τ, strongly decreases with increasing osmotic pressure $\Pi > \Pi^*$, as shown by the closed points in Fig. 1(e). We hypothesize that this behavior reflects the dynamics of the fluid flow through the capsule shell; for the capsule to buckle, a volume ΔV^* of fluid must be ejected from its interior. The time delay can then be estimated as $\tau = \Delta V^*/Q$ [34], where both ΔV^* and Q, the volumetric rate of fluid ejection from the capsule interior, are functions of δ/h_0. We calculate ΔV^* for inhomogeneous shells using shell theory and validate the calculations with numerical simulations; the fluid ejection rate Q follows from integrating Darcy's law over the surface of the capsule geometry shown in Fig. 1(a) [25]. Combining these results, we obtain

$$\tau \approx \frac{V_0}{Q_0}\sqrt{\frac{3(1-\nu)}{1+\nu}}\frac{h_0}{R_0}\left(1-\frac{\delta}{h_0}\right)^2, \tag{1}$$

where $Q_0 \equiv 4\pi R_0^2 \Pi k/\mu h_0$ and k is the shell permeability. For the inhomogeneous capsules, characterized by $\delta/h_0 \approx 0.2$, we thus expect $\tau/h_0^2 \approx 0.8\mu/k\Pi$; our experimental measurements of τ allow a direct test of this prediction. Above Π^*, the data collapse when τ is rescaled by h_0^2, as shown by the closed points in Fig. 1(e), consistent with our expectation; moreover, by fitting these data [black line in Fig. 1(d)], we obtain an estimate for the shell permeability, $k \approx 7 \times 10^{-24}$ m^2. We use optical microscopy to directly measure the rate at which the capsule volume decreases immediately after the onset of buckling [25]; this gives an independent measure of the shell permeability. We find $k \approx 2 \times 10^{-24}$ m^2 (Fig. S8, in Ref. [25]), in good agreement with the fit shown in Fig. 1(e); this further confirms the validity of Eq. (1).

To test the applicability of this picture to even more inhomogeneous capsules, we measure τ for capsules polymerized at different t_w; these have shells with $h_0/R_0 = 0.017$ and δ/h_0 ranging from 0.2 up to 0.84. We impose a fixed osmotic pressure $\Pi \approx 0.86$ MPa $> \Pi^*$. We observe that τ decreases only slightly with increasing $t_w < 10^3$ s; however, as t_w is increased above this value, τ drops precipitously over 1 order of magnitude, as shown by the

points in Fig. 1(f). To quantitatively compare these data to Eq. (1), we estimate the dependence of δ/h_0 on t_w using lubrication theory; we validate this calculation using direct measurements of δ/h_0 for capsules prepared at varying t_w [25,35]. Remarkably, we find good agreement between our data and Eq. (1), with $k \approx 3.5 \times 10^{-24}$ m^2, as shown by the black line in Fig. 1(f); in particular, this simple picture captures the strong decease in τ at $t_w \sim 10^3$ s, with a shell permeability consistent with our independent measurements (Fig. S8, in Ref. [25]). While these results do not rule out other possible functional forms of τ, they further suggest that the time delay before the onset of buckling can be understood by combining shell theory with Darcy's law for flow through the capsule shell, even for very inhomogeneous shells.

The shell thickness inhomogeneity may continue to guide the development of deformations in a capsule after it buckles. To explore this possibility, we use optical microscopy to monitor the evolution of the capsule morphologies after the onset of buckling. Slightly inhomogeneous capsules typically buckle through the sudden formation of a single circular indentation. As this indentation grows over time, its perimeter eventually sharpens into straight ridges connected by 2-3 vertices [14,19,36]; this folding pathway is exemplified by capsules polymerized *in situ*, characterized by $\delta/h_0 \approx 0.2$, as shown in Fig. 2(a). This sharpening reflects the unique physics of thin shells: because it is more difficult to compress the capsule shell than it is to bend it, localizing compressive deformations only along sharp lines and points on the capsule surface requires less energy than uniformly compressing the shell [37]. Interesting differences arise for very inhomogeneous capsules polymerized after $t_w = 1$ day, characterized by
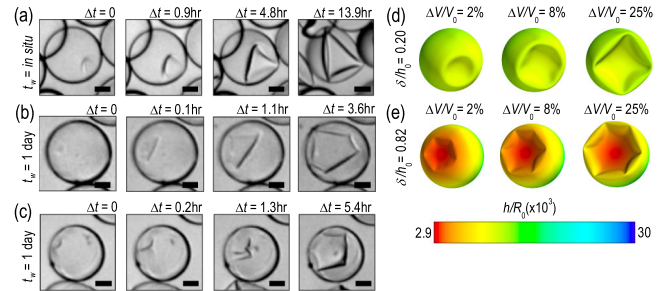

FIG. 2 (color online). Folding pathways for different shell inhomogeneities. (a)–(c) Optical microscope images exemplifying buckling at $\Pi \approx 0.86$ MPa of (a) slightly inhomogeneous capsules polymerized *in situ* ($t_w \approx 0$), with $\delta/h_0 \approx 0.2$, (b)–(c) very inhomogeneous capsules polymerized after a wait time $t_w = 1$ day, with $\delta/h_0 \approx 0.84$. Very inhomogeneous capsules buckle through the formation of either (b) one single indentation or (c) two indentations. Δt is the time elapsed after buckling. Scale bars are 35 μm. (d)–(e) Examples of simulated shells with similar geometries as the capsules shown in (a)–(c), for varying fractional volume reduction $\Delta V/V_0$. Color scale indicates the spatially varying shell thickness.
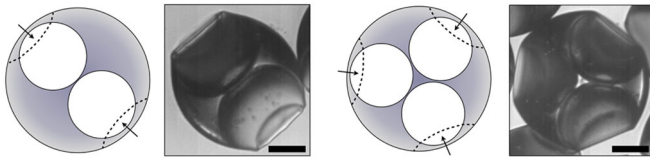
FIG. 3 (color online). Colloidal capsules with two or three spherical interior compartments, schematized in left panels, buckle at "weak spots" (arrows). This forms shapes with two or three equally spaced circular indentations after buckling (right panels). Scale bars are 100 μm.

$\delta/h_0 \approx 0.84$. The initial folding pathway is similar; however, the perimeters of the indentations formed in these capsules sharpen into straight ridges connected by 4-5 vertices, more than in the slightly inhomogeneous case, as shown in Fig. 2(b). Moreover, surprisingly, roughly 30% of the very inhomogeneous capsules begin to buckle through the formation of one, then two, adjacent indentations, as exemplified in Fig. 2(c). The perimeters of these indentations grow over time, eventually meeting, coalescing, and sharpening into straight ridges connected by 4-5 vertices [Fig. 2(c)]. These observations directly demonstrate that the deformations of a capsule after it buckles are sensitive to the shell inhomogeneity.

To gain insight into this behavior, we perform numerical simulations of two different shells, a slightly inhomogeneous shell with $\delta/h_0 = 0.20$, and a very inhomogeneous shell with $\delta/h_0 = 0.82$, similar to the experimental capsules. As the shell volume is reduced below $V_0 - \Delta V^*$, both shells buckle through the formation of a single indentation centered at the thinnest part of the shell, as shown in the leftmost panels of Figs. 2(d) and 2(e). As ΔV increases, this indentation grows and its edges sharpen. We find that the indentations formed in the very inhomogeneous shells begin to sharpen at smaller $\Delta V/V_0$, and ultimately develop more vertices than those formed in more homogeneous shells [Figs. 2(d) and 2(e)] [25]. These results qualitatively agree with our experimental observations [Figs. 2(a)–2(c)], further confirming that after the onset of buckling, the folding pathway of a shell depends on the inhomogeneity. However, in contrast to the experimental capsules [Fig. 2(c)], we do not systematically observe the formation of adjacent indentations in the simulations on very inhomogeneous shells [38]. This presents a puzzle requiring further inquiry.

Our capsules may be used to guide colloidal self-assembly; for example, a colloidal particle can spontaneously bind to the indentation formed during buckling through a lock-and-key mechanism [39]. This mechanism is typically applied to a homogeneous colloidal particle, which buckles through the formation of a single indentation at a random position on its surface. We apply our findings to create multiply indented capsules having two-fold or threefold symmetry. To do this, we form double emulsions with two or three inner droplets of radii larger than half the radius of the outer droplet. Consequently, the inner droplets pack closely to form dimers or trimers [40], as shown schematically in Fig. 3. The double emulsions are then polymerized, forming solid capsules with two or three spherical compartments in their interiors, and two or three equally spaced "weak spots" in the capsule shell [arrows in Fig. 3]. When exposed to a sufficiently large osmotic pressure, these capsules buckle through the formation of multiple, equally spaced indentations at the weak spots, as shown in Fig. 3. This approach is thus a versatile way to create capsules of desired symmetries, and extends the range of structures that can be used for lock-and-key colloidal assembly.

[1] S. S. Datta, H. C. Shum, and D. A. Weitz, Langmuir **26**, 18612 (2010).

[2] A. Fery, F. Dubreuil, and H. Mohwald, New J. Phys. **6**, 18 (2004).

[3] C. Quilliet, C. Zoldesi, C. Riera, A. van Blaaderen, and A. Imhof, Eur. Phys. J. E **27**, 13 (2008).

[4] D. Vella, A. Ajdari, A. Vaziri, and A. Boudaoud, J. R. Soc. Interface **9**, 448 (2011).

[5] D. A. Fletcher and R. D. Mullin, Nature (London) **463**, 485 (2010).

[6] E. Katifori, S. Alben, E. Cerda, D. R. Nelson, and J. Dumais, Proc. Natl. Acad. Sci. U.S.A. **107**, 7635 (2010).

[7] W. A. Nash, *Hydrostatically Loaded Structures* (Pergamon, New York, 1995).

[8] P. T. Pederson and J. J. Jensen, Thin-Walled Struct. **23**, 41 (1995).

[9] P. Kearey and F. J. Vine, *Global Tectonics* (Blackwell, Oxford, 1996).

[10] J. W. Hutchinson, J. Appl. Mech. **34**, 49 (1967).

[11] A. M. A van der Heijden, *W. T. Koiter's Elastic Stability of Solids and Structures (lecture notes).* (Cambridge University Press, Cambridge, England, 2009).

[12] G. A. Vliegenthart and G. Gompper, New J. Phys. **13**, 045020 (2011).

[13] S. Knoche and J. Kierfeld, Phys. Rev. E **84**, 046608 (2011).

[14] A. Vaziri and L. Mahadevan, Proc. Natl. Acad. Sci. U.S.A. **105**, 7913 (2008).

[15] D. N. Pinder. J. Theor. Biol. **34**, 407 (1972).
[16] M. A. Greenfield, L. C. Palmer, G. Vernizzi, M. Olvera de la Cruz, and S. I. Stupp, J. Am. Chem. Soc. **131**, 12 030 (2009).
[17] A. Touhami, B. Nysten, and Y. F. Dufresne, Langmuir **19**, 4539 (2003).
[18] F. Julicher and R. Lipowsky, Phys. Rev. Lett. **70**, 2964 (1993).
[19] L. Pauchard and S. Rica, Philos. Mag. B **78**, 225 (1998).
[20] V. Papadopoulos and M. Papadrakakis, Comput. Methods Appl. Mech. Eng. **194**, 1405 (2005).
[21] G. Vernizzi, R. Sknepnek, and M. Olvera de la Cruz, Proc. Natl. Acad. Sci. U.S.A. **108**, 4292 (2011).
[22] M. A. Krenzke and R. M. Charles, *The Elastic Buckling Strength of Spherical Glass Shells*, David Taylor Model Basin Report No. 1759, 1963.
[23] D. Bushnell, AIAA J. **5**, 1455 (1967).
[24] S. H. Kim, J. W. Kim, J. C. Cho, and D. A. Weitz, Lab Chip **11**, 3162 (2011).
[25] See Supplemental Material at http://link.aps.org/supplemental/10.1103/PhysRevLett.109.134302 for details of experimental procedures, analytical calculations, and numerical simulations.
[26] A. Fernandez-Nieves, V. Vitelli, A. S. Utada, D. R. Link, M. Marquez, D. R. Nelson, and D. A. Weitz, Phys. Rev. Lett. **99**, 157801 (2007).
[27] Each batch is characterized by a range of waiting times, with an average value t_w [25].
[28] The capsules produced *in situ* still correspond to some small, finite value of t_w, e.g., due to the droplet advection within the device.
[29] We measure the capsule geometric properties using either SEM or confocal microscopy of fluorescent capsules.
[30] T. H. Lin, W. H. Huang, I. K. Jun, and P. Jiang, Chem. Mater. **21**, 2039 (2009).
[31] S. H. Kim, S. J. Jeon, and S. M. Yang, J. Am. Chem. Soc. **130**, 6040 (2008).
[32] The spread in Π^* likely reflects the structural variability of the capsules.
[33] L. D. Landau and E. M. Lifshitz, *Theory of Elasticity* (Elsevier, New York, 1986), 3rd ed.
[34] The fluid ejection is resisted by the compressive stress in the shell; however, this stress can be omitted from Darcy's law for the range of Π studied here ([25] and D. Vella (private communication).
[35] P. G. Kim and H. A. Stone, Europhys. Lett. **83**, 54 001 (2008).
[36] D. Vella, A. Ajdari, A. Vaziri, and A. Boudaoud, Phys. Rev. Lett. **107**, 174301 (2011).
[37] T. A. Witten, Rev. Mod. Phys. **79**, 643 (2007).
[38] We observe this phenomenon for the inhomogeneous capsules buckled over a range of $\Pi \approx 0.5$–5 MPa, and do not observe it for the more homogeneous shells buckled at large pressures $\Pi \approx 10$ MPa; this suggests that it is not simply a function of the rate at which the capsule volume is reduced [12].
[39] S. Sacanna, W. T. M. Irvine, P. M. Chaikin, and D. J. Pine, Nature (London) **464**, 575 (2010).
[40] S. H. Kim, H. Hwang, C. H. Lim, J. W. Shim, and S. M. Yang, Adv. Funct. Mater. **21**, 1608 (2011).